ORIGINAL PAPER

A Comparison Between Monolithic and Wire Gauze Structured Catalytic Reactors for CH₄ and CO Removal from Biogas-Fuelled Engine Exhaust

P. J. Jodłowski · R. Gołąb · J. Kryca ·
A. Kołodziej · M. Iwaniszyn ·
S. T. Kolaczkowski · J. Łojewska

Abstract The application of the wire gauzes as the catalytic supports can provide a number of advantages in biogas exhaust abatement. In this paper, a model of wire gauze structured reactor for biogas exhaust removal is proposed and model based calculations are performed to compare the wire gauze catalytic reactor with the classic monolith. The modelling bases on kinetic data experimentally obtained in a small-scale tubular reactor for cobalt and palladium (as reference) oxide catalysts doped with promoters (Ce, Pd). The heat and mass transfer characteristics of the wire gauze reactor are taken from the former studies by the authors. The simulations show that for assumed reactor parameters, a combination of the promoted cobalt oxide catalyst and the wire gauze support can give high conversion of methane and carbon monoxide.

Keywords Biogas · Modelling · Biogas engines · Metal oxides catalyst

P. J. Jodłowski (✉) · R. Gołąb · J. Kryca · J. Łojewska
Faculty of Chemistry, Jagiellonian University, Ingardena 3, 30-060 Kraków, Poland
e-mail: przemyslaw.jodlowski@uj.edu.pl

A. Kołodziej
Faculty of Civil Engineering, Opole University of Technology, Katowicka 48, 45-061 Opole, Poland

A. Kołodziej · M. Iwaniszyn
Institute of Chemical Engineering of the Polish Academy of Sciences, Bałtycka 5, 44-100 Gliwice, Poland

S. T. Kolaczkowski
Department of Chemical Engineering, University of Bath, Claverton Down, Bath BA27AY, UK

List of symbols

|	
a	Specific surface area, m^{-1}
C_p	Heat capacity, $J\ mol^{-1}\ K$
C_A, C_{AS}	Reactant A concentration in bulk gas, at the surface, respectively; $mol\ m^{-3}$
D_h	Hydraulic diameter, m
E_a	Apparent activation energy, $J\ mol^{-1}$
h	Heat transfer coefficient, $W\ m^{-2}\ K$
ΔH_R	Heat of reaction, $J\ mol^{-1}$
k_r	Reaction rate constant, units dependent on R_A
k_C	Mass transfer coefficient of species A, $m\ s^{-1}$
k_∞	Apparent pre-exponential rate constant, $m\ s^{-1}$
L	Reactor length, m
L^*	Dimensionless reactor length for the thermal entrance region
L^{*M}	Dimensionless reactor length for the mass transfer entrance region
Pr	Prandtl number
Re	Reynolds number
R_g	Universal gas constant, $8.314\ J\ mol^{-1}\ K$
$(-R_A)$	Reaction rate expressed for substrate A at catalyst external surface, units vary
Sc	Schmidt number
Sh	Sherwood number
T, T_S	Temperature of bulk gas, catalyst surface, respectively, K
v_m	Mean mass average velocity in a duct, $m\ s^{-1}$
z	Reactor axis, m
η	Effectiveness factor for catalyst
ρ	Mass density, $kg\ m^{-3}$

1 Introduction

Nowadays, biomass utilization is becoming more and more problematic, due to its complex composition. Although the

idea of the gasification of renewable sources such as forestry residue and municipal wastes is not novel, in practice waste storage rather than its utilization prevails. One possible application of biomass waste is gasification to obtain the flammable gas containing H_2, CO and CH_4. The biogas may then be used as a fuel in either a biogas engine or turbine to produce energy at a local level [1]. During the energy production via biogas combustion, biogas engine emits a range of pollutants such as NO_x, CO, CH_4 and also some volatile organic compounds (VOCs), which must be cleaned to a level regulated by the European standards for waste incineration plants (Waste Incineration Directive, 2000/76/EC).

Although there are a few possible ways of gaseous pollutants abatement, catalytic removal seems to be the most efficient in many applications (e.g. automotive or energetics). Ceramic or metallic monoliths with noble metals as an active material are the most ubiquitous catalytic reactors due to their low flow resistance and usually sufficient mass transport properties. However, the so-called "short channel structures" working in a developing laminar flow regime show much more enhanced mass and heat transport accompanied with a relatively low flow resistance, which makes them good candidates for the biogas engines cleaning installations [2, 3]. Among them, wire gauzes have been demonstrated to be able to shorten reactor length by several times when comparing with the ceramic monoliths [4]. In spite of the fact that the idea of wire gauze-based structured reactor is not new and has been developed for ammonia oxidation to nitric acid [5], the literature data describing heat [6, 7] and mass [3] transfer phenomena of wire gauzes are scarce.

In this study, a reactor composed of wire gauzes with a catalyst deposited on them, for the abatement of trace contaminants gases from the biogas-fuelled engines, is modelled and compared with a classic monolithic reactor. The sketch of the reactor arrangements is presented in Fig. 1 together with the wire gauze internal assumed for the modelling and experimentally studied before [8, 9]. A series of metal oxides-based structured catalysts were prepared and tested in carbon monoxide and methane catalytic combustion (CC). The kinetic data of CO and CH_4 CC were experimentally derived using a small-scale test tubular reactor.
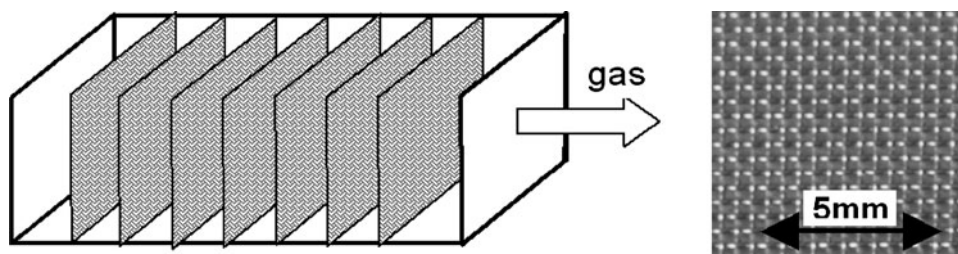
2 Experimental

2.1 Catalyst Preparation

Preparation of metal oxide catalyst on stainless steel sheets (00H20J5, Strzemieszyce, Poland; composition: Cr: 20.37 %, Al: 5.17 % and also Mn: 0.25 %, Ni: 0.16 %, Cu: 0.034 %, Co: 0.021 %) was performed in several steps: (a) steel support pre-calcination, (b) primer deposition, (c) coating deposition and (d) catalyst precursor deposition.

(a) *Steel support pre-calcination* in order to remove the superficial impurities the stainless steel sheets were first cleaned ultrasonically, cleaned in alkaline solution and then rinsed in distilled water. To form an alumina layer on the steel surface the sheets were calcined at 1,000 °C for 10 h. It was proved that this kind of treatment causes alumina whiskers growing on the stainless sheet support containing aluminium [10].

(b) *Primer deposition* to improve adherence of a washcoat layer, the primer layer was deposited. The stainless steel sheets were dipped in the boehmite solution obtained using Yoldas method [11], withdrawn with controlled speed 3 cm min^{-1} and dried at room temperature.

(c) *Coating deposition* to obtain the γ-Al_2O_3, the $Al(OH)_3$ powder (Sigma-Aldrich 23,918-6) was calcined at 700 °C for 6 h. Thus obtained alumina was dispersed in HNO_3 aqueous solution in the following proportions [10]: $HNO_3/Al_2O_3 = 2.16$ mmol g^{-1}, $H_2O/Al_2O_3 = 3.2$ g g^{-1}. The solution was then vigorously stirred at 18 °C in a closed vessel for 16 h. The precoated supports were dipped in the alumina solution and then withdrawn with control speed 3 cm min^{-1}. The steel supports pretreated in this way were then dried in a ventilated oven at 500 °C for 3 h with the temperature ramp of 5 °C min^{-1}.

(d) *Catalyst precursor deposition* a series of composite oxide catalysts were prepared using an impregnation method. The alumina coated metal sheets were immersed into metal-nitrate(V) solution of various concentrations for 1 h. After impregnation the catalysts were dried in ambient conditions and then calcined in

Fig. 1 Scheme of the wire gauze reactor and a picture of the wire gauze modelled

500 °C for 3 h in a ventilated oven. The catalyst (metal oxide) percent in the deposited alumina layer, determined from XRF (Thermo QUANT'X) quantitative analyses, is presented in Table 1.

2.2 Kinetic Tests

Catalytic oxidation of CH_4 and CO was carried out in 4 mm I.D. tubular quartz reactor CATLAB (Hiden Analytical; cf. the manufacturer's web page http://www.hidenanalytical.com). The outlet gases were analyzed with the quadruple mass spectrometer and Thermo FT-IR spectrometer equipped with the Gasera PA101 photoacoustic gas analysis module. Atom mass to charge values, m/z, used to detect the oxidation products and substrates were as follows: methane (16), water (18), oxygen (32), carbon monoxide (28), carbon dioxide (44). Prior to the catalytic tests catalyst samples were oxidized in synthetic air flow (Airproducts) at 500 °C for 1 h. The reaction mixture contained 4,000 ppm CH_4 or 4,000 ppm CO in the synthetic air (calibration gas, Airproducts). The total flow rates of reaction mixtures were: 25 and 80 cm^3 min^{-1} during CH_4 and CO oxidation, respectively.

The kinetic parameters used for reactor modelling for both CC reactions considered are provided in Table 1. They were calculated based on the approximation of a tubular reactor model assuming first order kinetics for both reactions, which is discussed below. All the kinetic experiments were repeated 5 times and the average value was taken for the Arrhenius plot. The error of kinetic constant k estimation from a single kinetic experiment never exceeded 9 % referred to the average value at a given temperature.

3 Reactor Modelling

The plug-flow model of the wire gauze reactor, which was derived and experimentally confirmed in [8], neglected heat evolved during the reaction, thus also the energy

balance, due to extremely low concentration of VOCs. In this paper the model has been improved by introducing the energy balance. The more general discussion on the reactor modelling can be found for example in [12].

3.1 Material Balance Equations

The steady state material balance of reactant A in a heterogeneous catalytic reactor with the boundary conditions (B. C.) is as follows:

$$\frac{d(C_A v_m)}{dz} + a k_C (C_A - C_{AS}) = 0 \tag{1}$$
$$B.C. \quad z = 0 : \quad C_A = C_{A0}$$

In this model, homogeneous reactions are ignored. Mass transfer is balanced by the reaction at the catalyst surface:

$$k_C(C_A - C_{AS}) = \eta(-R_A) = \eta \, k_r C_{AS} \tag{2}$$

The term η, represents the effectiveness factor of catalyst. The effectiveness factor, η, and the Thiele modulus, ϕ, are described by Eqs. (3) and (4), respectively:

$$\eta = \frac{tgh(\phi)}{\phi} \tag{3}$$

$$\phi = l\sqrt{\frac{k_r}{D_{Ai}}} \tag{4}$$

The effectiveness factor and the Thiele modulus were calculated for each considered catalyst (Table 1). The characteristic dimension, l, i.e. the thickness of the porous catalyst layer, was determined from SEM photographs of the wire gauze samples and in each case $l \approx 20 \, \mu m$.

3.2 Energy Balance Equations

When considering the chemical reactions on the catalyst surface, especially those of high exothermic effect, the energy balance has to be introduced to reactor equations. The energy balance for the bulk and solid phases can be written, respectively:

Table 1 Catalyst composition, kinetic and transport parameters obtained for two test reactions: CH_4 and CO catalytic combustion, and for two catalyst carriers: monolith and wire gauze

Catalyst	Metal oxide content (wt%)			k_∞ (m s^{-1})		Ea (kJ mol^{-1})		η	
	Co_3O_4	PdO	CeO_2	CH_4	CO	CH_4	CO	CH_4	CO
Pd0.001	–	8	–	20.6	10.4	24.4	25.7	0.94	0.34
Co0.1	29	–	–	Inactive					
Co1	59	–	–	3.12	2.24	36.9	17.2	0.88	0.12
Co1Pd0.001	14	1	–	1.73	1.68	39.8	20.1	1.0	0.73
Co1Ce1	8	–	0.01	1.01	1.93	28.16	20.3	0.91	0.060

$$-v_m \rho C_p \frac{dT}{dz} + a \cdot h(T_S - T) = 0 \qquad (5)$$

$$B.C. \quad z = 0: \quad T = T_0$$

$$h(T_S - T) = -\Delta H_R \eta(-R_A) \qquad (6)$$

3.3 Reaction Kinetics

Palladium is the most commonly used catalyst for the methane oxidation [13]. It was proved, that the methane oxidation over Pd/Al_2O_3 strongly depends on oxygen content. However, under oxygen-rich conditions, the catalyst surface is fully covered with oxygen, thus the rate expression with respect to O_2 can be neglected [13]. When considering the reaction order with respect to CH_4, the order varies between 0.45 and 1.2 depending on the catalyst system. According to Lee and Trimm [13], the reaction order over Pd/Al_2O_3 in excess of oxygen equals unity.

Oxidation of carbon monoxide over the precious metals was a subject of surveys of many groups, and provided numerous kinetic behaviour patterns. The literature provides many mechanisms of CO oxidation including the Langmuir–Hinshelwood–Hougen–Watson (LHHW) mechanism for CO oxidation over alumina-supported platinum catalysts [14] as well as the Eley–Rideal mechanism over alumina-supported palladium catalyst [15], with a CO desorption as the rate limiting step. According to the literature data, CO desorption may become very slow below 450 K [15], which is not the case in our modelling. Within the temperature range of 200–400 °C the rate equation simplifies to the first order with respect to CO and zero order to O_2 [15].

3.4 Modelling Conditions

Two different types of catalyst support were modelled and compared: (a) wire gauzes, (b) classic monolithic support. The heat and mass transfer correlations applied during reactor modelling are presented in Table 2 together with the geometric parameters of the wire gauze and monolith.

The heat and mass transfer characteristics (Sh, Nu) were described using the so-called heat or mass dimensionless channel length L^{*H} (L^{*M}):

$$Nu = \frac{hD_h}{\lambda} = f(L^{*H}), \qquad L^{*H} = \frac{L}{D_h \mathrm{Re}\,\mathrm{Pr}} \qquad (7)$$

$$Sh = \frac{k_C D_h}{D_A} = f(L^{*M}), \qquad L^{*M} = \frac{L}{D_h \mathrm{Re}\,\mathrm{Sc}} \qquad (8)$$

The physical and chemical parameters of the gas mixture used during the modelling (e.g. density, viscosity, heat conductivity and heat capacity) were calculated at the local temperature of the gas phase.

3.5 Reactor Performance

In summary, the following modelling assumptions were applied:

- For the reaction: $CH_4 + 2O_2 \rightarrow CO_2 + 2H_2O$ the heat of reaction at the catalyst surface was calculated to be, $\Delta H^\circ_R = -803$ kJ mol^{-1},
- For the reaction: $CO + 0.5O_2 \rightarrow CO_2$ the heat of reaction at the catalyst surface was calculated to be, $\Delta H^\circ_R = -283$ kJ mol^{-1},
- Properties along the channel varied as a function of the local temperature,
- The inlet gas temperature was assumed to 673 K,
- The gas superficial velocity was assumed to 1 m s^{-1}; the corresponding Reynolds numbers are given in Table 2.

The modelling results for both methane and carbon monoxide combustion are presented in Fig. 2.

When analysing the kinetic results for both reactions, the external and internal mass transfer resistances are evidently significant. This results in low value of activation energy (Ea) (cf. Table 1), which is not surprising as the kinetic tests were performed in small tubular reactor where the steel sheets with deposited catalyst were randomly distributed. In this way, the kinetic parameters obtained should be treated as apparent and they will be used for exclusively simulations in order to compare different reactor internals and catalysts. Similar effects of mass transport limitations have already been reported for methane oxidation by a number of authors [19–21].

Table 2 Reactor assessment: geometric parameters of reactor internals, average Reynolds numbers used for modelling, heat and mass transfer correlations (gas velocity $v_m = 1$ m s^{-1})

Reactor internals	D_h (mm)	a (m^{-1})	Mesh/cpsi	Re	Heat and mass transfer equation	Ref.
Wire gauze	0.33	8,186	61.7	12	$Nu = \frac{2[(4/\pi)\cdot L^*]^{-1/2}}{[1+(Pr/0.0207)^{2/3}]^{1/4}}\left(0.270 \cdot (Pr \cdot L^*)^{-0.213}\right)$ $Sh = \frac{2[(4/\pi)L^{*M}]^{-1/2}}{[1+(Sc/0.0207)^{2/3}]^{1/4}}\left(0.270 \cdot (Sc \cdot L^{*M})^{-0.213}\right)$	[9, 16]
Monolith	2.15	1,339	100	80	$Nu = 3.608\left(1 + \frac{0.095}{L^*}\right)^{0.45}$ $Sh = 3.608\left(1 + \frac{0.095}{L^{*M}}\right)^{0.45}$	[17, 18]
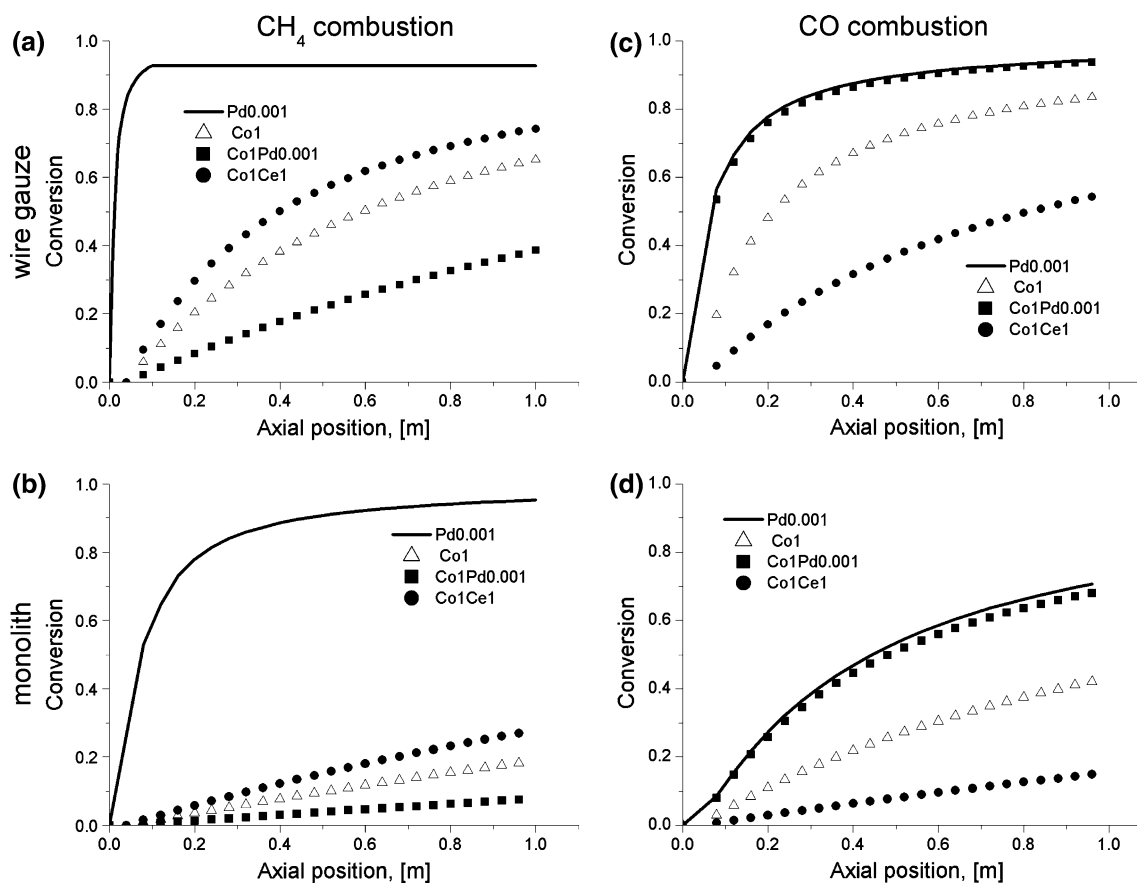
Fig. 2 Comparison of reactor types and catalysts: conversion versus axial position

The results of the simulations performed for methane and carbon monoxide combustion over the cobalt and palladium catalysts applied for the wire gauze and monolithic reactors are presented in Fig. 2a–d. In order to assess the performance of the reactors, maximum achieved conversions are compared at the maximum reactor length used for modelling. The differences between the considered reactor internals are substantial. It can be noted that the wire gauze internals enables to achieve almost 100 % conversion in much shorter reactor than the monolith, which is especially evident for the Pd0.001 catalyst (8 wt%) during methane combustion. The most important factor influencing this is higher catalyst amount arising directly from higher specific surface area of wire gauze. The impact of better mass transfer intensity is also significant, especially for very fast catalytic reactions (i.e. for very active catalysts).

A comparison of the gas hourly space velocity (GHSV) necessary to achieve final conversion of 50 % is presented in Table 3. As it can be noted, for all the catalysts considered the GHSV of the gauze reactor is 6 till 8 times higher comparing with monolithic reactor with the same catalyst. Upon referring to the ratio of specific surface

Table 3 Comparison of the gas hourly space velocity (GHSV, 1/h) assuming final conversion X = 0.5

Catalyst	Methane combustion		CO combustion	
	Wire gauze	Monolith	Wire gauze	Monolith
Pd0.001	300,000	51,429	60,000	7,826
Co1	6,000	938	16,363	2,609
Co1Pd0.001	2,368	375	51,429	7,059
Co1Ce1	9,000	1,286	4,286	652

areas amounting to 6.1, the impact of better mass transfer (of the wire gauze reactor) is distinct.

It should also be inferred from Fig. 2 that the catalysts are very different in their performances. The outstanding activity of the Pd0.001 reference sample is confirmed. However, high surface area and high mass transport of wire gauzes allows for exploitation of low-loaded Co1Ce1 catalyst in methane combustion. This catalyst exhibits similar activity to highly loaded cobalt sample Co1 (Fig. 2a). For the Co1Ce1 catalyst, 80 % conversion can be achieved in 1 m long reactor filled with wire gauzes, while for the monolith, the same conversion would require 4 m long

reactor (cf. Fig. 2a, b). During CO combustion, similar performances can be noted for the Pd0.001 catalyst (8 wt% PdO) and Co1Pd0.001 catalyst (1 wt% PdO). Again, Co1 catalyst performance in wire gauze reactor is worth emphasising.

The temperature distribution is not shown in this study. However, temperature increases inside the reactor due to heat evolved during the reaction (assuming negligible heat losses). The gas–solid temperature difference was significantly lower for the wire gauze reactor than for the monolith (on average, 7 vs. 83 K, respectively). This results in less hazardous overheating of the catalyst when using wire gauze support. The problem is of high importance for the methane CC due to high reaction heat.

A question arises about accuracy of the modelling performed. The model together with the transfer coefficients and the kinetic equation used (although for another catalyst composition and for combustion of n-hexane) was successfully tested in a large laboratory-scale reactor (up to 10 $Nm^3 h^{-1}$). The experimental results were in excellent agreement with the modelling; the details are provided in [8, 22].

The reactor evaluations and comparisons presented here should be treated as rather preliminary. The kinetic data were derived using artificial air thus the influence of other components appearing in the exhaust (H_2O, N_2, O_2, CO_2) may influence the results to a certain degree. The mass transfer limitations which occur during experiments were already mentioned. The modelling is, in fact, strictly valid only for the assumed reactor parameters such as temperature, gas velocity, etc. (see model assumptions above and Table 2). However, the results indicate on a very promising way for the CC intensification: wire gauzes display large specific surface area and intense mass transfer (see Table 2) which is coupled with layered catalyst of high activity and high efficiency factor (due to thin layers, see Table 1).

3.6 Conclusive Remarks

The simulations presented here proved decisive for the evaluation of the catalytic reactor inner structure. It has been demonstrated that both catalyst activity and reactor structured internals play important roles in tuning the overall reactor performance. Indeed, it has been demonstrated that the wire gauze internals even with metal oxide (non-nobel) catalysts offer undeniable benefits, which can be exploited in the CC applications in biogas engines. The wire gauze internals enable significant reactor shortening compared with ceramic monolith, by 2 till 10 times depending on the final conversion required and the catalyst used.

Although low loaded cobalt oxide catalysts did not show any methane conversion, small addition of cerium (0.01 wt%) gave a profound enhancement of cobalt catalyst activity. It is also worth noting that during CO combustion low loaded cobalt oxide catalyst (<10 wt%) enabled to reduce the amount of Pd by 8 times achieving the same conversion.

Remarkable results predicted for the wire gauze reactor by the reliable modelling show this reactor design as promising for many applications, especially environmental ones.

References

1. Knoef HAM (2005) Handbook of biomass gasification. BTG biomass technology group BV, Enschede
2. Kołodziej A, Łojewska J, Ochońska J, Łojewski T (2011) Short-channel structured reactor: experiments versus previous theoretical design. Chem Eng Process 50:869–876
3. Kołodziej A, Łojewska J (2007) Short-channel structured reactor for catalytic combustion: design and evaluation. Chem Eng Process 46:637–648
4. Kołodziej A, Łojewska J (2007) Prospect of compact afterburners based on metallic microstructures. Design and modelling. Top Catal 42–43:475–480
5. Twigg MV, Webster DE (2005) In: Cybulski A, Moulijn JA (eds) Structured catalysts and reactors, 2nd edn. CRC Press, New York
6. Satterfield CN, Cortez DH (1970) Mass transfer characteristics of woven-wire screen catalysts. Ind Eng Chem Fundam 9:613–620
7. Mobarak AA, Abdo MSE, Hassan MSN, Sedahmed GH (2000) Mass transfer behaviour of a flow-by fixed bed electrochemical reactor composed of a vertical stack of screens under single and upward two phase flow. J Appl Electrochem 30:1269–1276
8. Kołodziej A, Łojewska J (2009) Mass transfer for woven and knitted wire gauze substrates: experiments and modelling. Catal Today 147S:120–124
9. Kołodziej A, Łojewska J, Jaroszyński M, Gancarczyk A, Jodłowski P (2012) Heat transfer and flow resistance for stacked wire gauzes: experiments and modelling. Int J Heat Fluid Flow 33:101–108
10. Valentini M, Groppi G, Cristiani C, Levi M, Tronconi E, Forzatti P (2001) The deposition of Al_2O_3 layers on ceramic and metallic supports for the preparation of structured catalysts. Catal Today 69:307–314
11. Brinker CJ, Scherer GW (1990) Sol–gel science: the physics and chemistry of sol–gel processing. Academic Press, New York
12. Salmi TO, Mikkola JP, Warna JP (2011) Chemical reaction engineering and reactor technology. CRC Press, Boca Raton
13. Lee D, Trimm H (1995) Catalytic combustion of methane. Fuel Process Technol 42:339–359
14. Hayes RE, Kolaczkowski ST (1997) Introduction to catalytic combustion. Gordon and Breach Science Publishers, Reading
15. Close JS, White JM (1975) On the oxidation catalyzed of carbon monoxide by palladium. J Catal 198:185–198

16. Kołodziej A, Łojewska J (2009) Experimental and modelling study on flow resistance of wire gauzes. Chem Eng Process 48:816–822

17. Hayes RE, Kolaczkowski ST (1999) A study of Nusselt and Sherwood numbers in a monolith reactor. Catal Today 47:295–303

18. Hawthorn RD (1974) Afterburner catalysts effects of heat and mass transfer between gas and catalyst surface. AIChE Symp Ser 70:428

19. Cullis CF, Willat BM (1984) The inhibition of hydrocarbon oxidation metal catalysts over supported. J Catal 86:187–200

20. Hayes RE, Kolaczkowski ST, Li PKC, Awdry S (2001) The palladium catalysed oxidation of methane: reaction kinetics and the effect of diffusion barriers. Chem Eng Sci 56:4815–4835

21. Kolaczkowski ST, Thomas WJ, Titiloye J, Worth DJ (1996) Catalytic combustion of methane in a monolith reactor: heat and mass transfer under laminar flow and pseudo-steady-state reaction conditions. Combust Sci Technol 118:79–100

22. Kołodziej A, Łojewska J, Tyczkowski J, Jodłowski P, Redzynia W, Iwaniszyn M, Zapotoczny S, Kuśtrowski P (2012) Coupled engineering and chemical approach to the design of a catalytic structured reactor for combustion of VOCs: cobalt oxide catalyst on knitted wire gauzes. Chem Eng J 200–202:329–337